Published online 19 May 2008 *Nucleic Acids Research, 2008, Vol. 36, No. 11* ***3765–3780***
doi:10.1093/nar/gkn120

Structural polymorphism within a regulatory element of the human *KRAS* promoter: formation of G4-DNA recognized by nuclear proteins

Susanna Cogoi[1], Manikandan Paramasivam[1], Barbara Spolaore[2] and Luigi E. Xodo[1,*]

[1]Department of Biomedical Science and Technology, School of Medicine, Ple. Kolbe 4, 33100 Udine and [2]CRIBI Biotechnology Centre, University of Padova, Viale G. Colombo 3, 35121 Padova, Italy

Received January 21, 2008; Revised March 3, 2008; Accepted March 4, 2008

ABSTRACT

The human *KRAS* proto-oncogene contains a critical nuclease hypersensitive element (NHE) upstream of the major transcription initiation site. In this article, we demonstrate by primer-extension experiments, PAGE, chemical footprinting, CD, UV and FRET experiments that the G-rich strand of NHE (32R) folds into intra-molecular G-quadruplex structures. Fluorescence data show that 32R in 100 mM KCl melts with a biphasic profile, showing the formation of two distinct G-quadruplexes with T_m of ~55°C (Q_1) and ~72°C (Q_2). DMS-footprinting and CD suggest that Q_1 can be a parallel and Q_2 a mixed parallel/antiparallel G-quadruplex. When dsNHE (32R hybridized to its complementary) is incubated with a nuclear extract from Panc-1 cells, three DNA–protein complexes are observed by EMSA. The complex of slower mobility is competed by quadruplex 32R, but not by mutant oligonucleotides, which cannot form a quadruplex structure. Using paramagnetic beads coupled with 32R, we pulled down from the Panc-1 extract proteins with affinity for quadruplex 32R. One of these is the heterogeneous nuclear ribonucleoprotein A1, which was previously reported to unfold quadruplex DNA. Our study suggests a role of quadruplex DNA in *KRAS* transcription and provides the basis for the rationale design of molecular strategies to inhibit the expression of *KRAS*.

INTRODUCTION

KRAS is one of the most frequently mutated oncogenes detected in human cancer. It encodes for a guanine nucleotide (GTP/GDP)-binding protein acting as a signal transducer (1). The normal (wild-type) RAS protein is transiently activated by signals from cell receptors that promote the exchange of bound GDP with GTP. The protein returns to its inactivated state through the hydrolysis of GTP to GDP. It has been shown that the *KRAS* gene may harbour a number of point mutations resulting in aminoacid substitutions (in particular, at codons 12, 13 and less frequently at codons 59, 61 and 63) that yield a protein with a reduced capacity to hydrolyze GTP (2–4). As a result, the mutated RAS protein remains locked in the activated state, transmitting constitutively signals for cell proliferation to the nucleus, via the MAP-kinase cascade (5). Activating *KRAS* mutations are most prevalent in pancreatic (60%), biliary tract (33%), colorectal (32%) and lung (19%) carcinomas (6). Due to its role in the pathogenesis of cancer, *KRAS* is an ideal target for anticancer drugs. Several anti-*KRAS* molecular strategies have been proposed: (i) inhibition of *KRAS* expression by antisense, ribozyme and antigene oligonucleotides (7–11); (ii) blockade of RAS protein to anchor to the plasma membrane by farnesyl transferase inhibitors (12,13); (iii) inhibition of downstream effectors of the RAS proteins (14,15). The human *KRAS* gene is located in chromosome 12, at the 12p12.1 locus, and its promoter contains a polypurine nuclease hypersensitive element (NHE) that plays an essential role in transcription (16–18). Nuclease-hypersensitive sites rich in guanines are commonly found in the regulatory regions of eukaryotic genes and have been associated with non-B-DNA conformations (19). The most investigated nuclease-hypersensitive sequence is the one located in *CMYC*, upstream of the P1 promoter that controls 80–90% of transcription (20–22). Hurley and co-workers have demonstrated that the *CMYC* hypersensitive site adopts stable G-quadruplex (or G4-DNA) structures that seem to behave as a transcription repressor (21). These data strongly support the notion that certain nuclease hypersensitive sites can assume two possible conformations: a double-stranded, transcription-active form or a folded,

*To whom correspondence should be addressed. Tel: +39 0432 494395; Fax: +39 0432 494301; Email: lxodo@makek.dstb.uniud.it

Table 1. Oligonucleotides used in this study (5′ → 3′)

32R and mutant sequences[a]	
AGGGCGGTGTGGGAAGAGGGAAGAGGGGGAGG	32R
(FAM)AGGGCGGTGTGGGAAGAGGGAAGAGGGGGAGG(TAMRA)	Fa-32R-Ta
biotin-AGGGCGGTGTGGGAAGAGGGAAGAGGGGGAGG	B-32R
AGGGCGGTGTGGGAAGATTTAAGAGGGGGAGG	32R-3L
AGGGCGGTTTGGGAATAGGGAATAGGGGGAGG	32R-3T
AGTGCGGTGTGTGAAGAGTGAAGAGTGGGAGG	32R-4T
AGGGCGGTGTGGGAAGAGGGAAGAGGGTTAGG	32R-2T
AGCGCGGTGTGCGAAGAGCGAAGAGCGGGAGG	32R-4C
AGCCCGGTGTGCCAAGAGCCAAGAGCCGGAGG	32R-8C
ACCCCGGTGTCCCAAGACCCAAGACCCGGAGG	32R-12C
TGGGGAGGGTGGGGAGGGTGGGGAAGG	CMYC
CTGCCTCCCCCTCTTCCCTCTTCCCACACCGC	32Y
GCATTCTGATTACACGTATTACCTTCACTCCA	32deg
biotin-CGCACGCTTATTTGCCTCCCTGTTTAACTCTTCGGTGGTA	B-scram
RT-PCR primers	
CAGGAAGCAAGTAGTAATTGATGG	KRAS forward
TTATGGCAAATACACAAAGAAAGC	KRAS backward
CCCTTCATTGACCTCAACTACATG	GAPDH forward
TGGGATTTCCATTGATGACAAGC	GAPDH backward

[a]Fa, FAM; Ta,TAMRA; B, biotin.

transcription-inactive form. A similar picture was recently proposed for the murine *KRAS* gene that also contains a G-rich NHE in its promoter (23). Other promoter/enhancer sequences composed by multiple runs of guanines are structurally polymorphic. For instance, three overlapping G-rich sequences within the promoter of *BCL-2* form distinct G-quadruplex structures, each characterized by a different loop topology (24); a polypurine tract of the hypoxia-inducible factor 1-α promoter forms a parallel quadruplex (25); G-rich regions forming G4-DNA are present in promoter/enhancer sequences of *VEGF* (26); the *PDGF*-A gene is regulated by multiple promoter and silencer elements that are CG-rich and exhibit a single-stranded folded character (27); C*KIT* (28) and muscle-specific human sarcomeric mitochondrial creatine kinase (sMtCK) (29) contain sequences that form quadruplex structures. This leads to the suggestion that G4-DNA in the control region of the genes may contribute to the regulation of gene expression (30,31).

In this work, we demonstrate that the G-rich strand of NHE, located in the human *KRAS* promoter, can fold into a dynamic intra-molecular G-quadruplex that can assume two distinct conformations for which we propose, on the basis of circular dichroism (CD) and DMS-footprinting data, folding topologies with three and four loops. Pull-down assays were used to isolate from a pancreatic adenocarcinoma nuclear extract proteins that have affinity for the G-quadruplex of 32R. LC-MS/MS of in-gel tryptic digests of these proteins allowed the identification of poly[ADP-ribose] polymerase I (PARP-1), ATP-dependent DNA helicase 2 subunit 1 (Ku70) and heterogeneous nuclear ribonucleoprotein A1 (hnRNP A1). PARP-1 and the dimer Ku70–Ku83 bind also duplex NHE (dsNHE). The proteins of the hnRNP family are of particular interest, as some of them show unfolding properties against G4-DNA [for a comprehensive review see ref. (32)]. The observation that *KRAS* transcription in Panc-1 cells is reduced by TMPyP4 (but not by TMPyP2), a cationic G4-DNA stabilizing ligand, confirm the notion that folded G-quadruplex structures within critical promoter region behaves, indeed, as a transcription repressor. The implications of these findings in the regulation of *KRAS* transcription as well as in the development of new molecular approaches to specifically inhibit oncogenic *KRAS* are discussed.

MATERIALS AND METHODS

Oligonucleotides and porphyrins

The oligonucleotides (sequences in Table 1) were obtained from Sigma-Proligo (Paris, France). They were purified by electrophoresis using a denaturing 20% polyacrylamide gel (acrylamide: bisacrylamide, 19 : 1) in TBE, 7 M urea, 55°C. The bands were excised from the gel and eluted in water. The DNA solutions were filtered (Ultrafree-DA, Millipore, Billerica, MA) and precipitated. The concentration of each DNA was determined from the absorbance at 260 nm in milli Q water, using as extinction coefficients 7500, 8500, 15 000 and 12 500 $M^{-1}cm^{-1}$ for C, T, A and G, respectively. Dual-labelled 32R [5′ end with fluorescein (FAM), 3′end with tetramethylrhodamine (TAMRA)] was HPLC purified. Porphyrins TMPyP2, TMPyP3 were purchased from Porphyrin Systems (Lübeck, Germany), while TMPyP4 from Sigma (Milan, Italy).

Polymerase stop assay

A DNA fragment of 80 bp, containing the NHE sequence (access number L00044 bases 228–306), was cloned in plasmid pBSKS+ at SmaI, in the orientation that the polypurine strand of NHE was the template for T3-primer extension reactions. Vector pBSKS-NHE (15 nm) was denatured at 95°C in the presence of NaOH (100 mM) then neutralized with an equivalent amount of HCl. Following this treatment, the vector was added with T3 primer for DNA polymerase I (7.5 nm), 100 mM KCl,

100 nm TMPyP4 and Klenow buffer (New Englands Biolabs, Ipswich, MA). After 1 or 3 h of incubation at 50°C, the primer extension reactions were carried out for 30 min at 37°C, by adding 10 mM DTT, 100 μM dATP, dGTP, dTTP, 1 μM [α-^{32}P] dCTP (7.4 Bq) and 3.75 U DNA Polymerase I (large Klenow fragment) (New Englands Biolabs). The reactions were stopped by adding an equal volume of stop buffer (95% formamide, 10 mM EDTA, 10 mM NaOH, 0.1% xylene cyanol, 0.1% bromophenol blue). The products were separated on a 15% polyacrylamide sequencing gel prepared in TBE, 8 M urea. The gel was dried and exposed to autoradiography. Standard dideoxy sequencing reactions were performed to detect the points in which DNA polymerase I was arrested.

Circular dichroism, ultraviolet and fluorescence experiments

CD spectra were obtained using a JASCO J-600 spectropolarimeter equipped with a thermostatted cell holder. CD experiments were carried out with oligonucleotides (1 or 3 μM) in Tris 50 mM, pH 7.4, 100 mM KCl. Spectra were recorded in 0.5 cm quartz cuvette. A thermometer inserted in the cuvette holder allowed a precise measurement of the sample temperature. The spectra were calculated with J-700 Standard Analysis software (Japan Spectroscopic Co., Ltd, Tokyo, Japan) and are reported as ellipticity (millidegrees) versus wavelength (nanometres). Each spectrum was recorded three times, smoothed and subtracted to the baseline. UV measurements were obtained with a (Perkin–Elmer Spectrophotometer, Waltham, MA) equipped with a thermostatted cell holder. Spectra were recorded in 0.5 cm quartz cuvette containing 3 μM DNA solution.

Fluorescence measurements were carried out with a Microplate Spectrofluorometer System (Molecular Devices, Concorde, Canada) using a 96-well optical-bottom plate, in which each well contained 50 μl of 300 nm dual-labelled 32R in 50 mM Tris–HCl, pH 7.4, and lithium or potassium chloride as specified in the figure captions. The samples were overnight incubated at 37°C before measurements. The emission spectra were obtained setting the excitation wavelength at 475 nm, the cut-off at 515 nm and recording the emission from 500 to 650 nm. Fluorescence melting experiments were performed on a real-time PCR apparatus (iQ5, BioRad, Hercules, CA), using a 96-well plate filled with 50 μl solutions of dual-labelled 32R, prepared as described above. The protocol used for the melting experiments is the following: (i) equilibration step of 5 min at low temperature (20°C); (ii) stepwise increase of the temperature of 1°C/min for 76 cycles to reach 95°C. All the samples in the wells were melted in 76 min. After melting the samples were re-annealed, melted again to give the same melting curves.

Electrophoretic mobility shift assay (EMSA)

Oligonucleotides 32R, 32Y and 32deg were end-labelled with [γ-P^{32}]ATP and T4 polynucleotide kinase (30 pmol) and purified by denaturing polyacrylamide gel electrophoresis (PAGE). Duplex dsNHE was prepared annealing (10 min at 95°C and overnight at room temperature) a mixture containing equimolar amounts of radiolabelled 32R and complementary cold 32Y in 50 mM Tris–HCl, pH 7.4, 100 mM NaCl. To observe quadruplex formation, 32R was incubated overnight at 37°C in 50 mM Tris–HCl, pH 7.4, 140 (or 50) mM KCl, 10 mM $MgCl_2$. The samples were also incubated with and without TMPyP4, as specified in Figure 2. After incubation, the samples were loaded in a 15% native polyacrilamide gel in TB, containing 50 mM KCl in the gel and running buffer. After running, the gel was dried and exposed to autoradiography (Hyperfilm, GE Healthcare, Milan, Italy) for few hours.

DMS-footprinting and TMPyP4-photocleavage experiments

PAGE-purified oligonucleotide 32R (25 nm), end-labelled with [γ-^{32}P] ATP (GE Healthcare, Europe, GmbH) and polynucleotide kinase (New England Biolabs, MA, USA), was incubated overnight at 37°C, in 50 mM sodium cacodylate, pH 8, 1 mM EDTA, 0, 50 or 100 mM KCl, 1 μg sonicated salmon sperm DNA. Some DNA solutions were added with 50 or 100 nm TMPyP4. Dimethyl sulphate (DMS) dissolved in ethanol (DMS : ethanol, 1 : 10, vol/vol) was added to the DNA solution (1 μl to a total volume of 20 μl) and left to react for 5 min at room temperature. For photocleavage experiments, the DNA solutions containing 100 nm TMPyP4 were incubated in cacodylate buffer containing 100 mM KCl, and treated for 5, 10 or 15 min with white light from a Solaris 2 (J615) projector (150 W) at a fluence rate of 64 mW/cm^2. Both DMS and photocleavage reactions were stopped by the addition of 1 : 4 volume of Stop solution (1.5 M sodium acetate pH 7, 1 M β-mercaptoethanol, 1 μg/μl tRNA). DNA was precipitated with 4 volumes of ethanol and resuspended in piperidine 1 M. After cleavage at 90°C for 30 min, reactions were stopped by chilling in ice followed by precipitation with sodium acetate 3 M pH 5.2 and 3 volumes of ethanol. The DNA samples were resuspended in 90% formamide and 50 mM EDTA, denatured at 90°C and run for 2 h on a denaturing 20% polyacrylamide gel, prepared in TBE and 8 M urea, pre-equilibrated at 55°C in a Sequi-Gen GT Nucleic Acids Electrophoresis Apparatus (BioRad, CA, USA), which was equipped with a thermocouple that allows a precise temperature control. After running, the gel was fixed in a solution containing 10% acetic acid and 10% methanol, dried at 80°C and exposed to Hyperfilm MP (GE Healthcare) for autoradiography.

Preparation of nuclear protein extract and EMSA

Nuclear extracts were obtained as described by Abmayr and Workman (33). Briefly, 10 plates of 10-cm diameter of confluent Panc-1 cells were collected and resuspended in hypotonic buffer (10 mM HEPES, pH 7.9, 1.5 mM $MgCl_2$, 10 mM KCl, 0.2 mM PMSF, 0.5 mM DTT, 5 mM NaF, 1 mM Na_3VO_4). Swollen cells were homogenized with a Dounce homogenizer and the nuclei, pelleted by centrifugation, were resuspended in low-salt buffer (20 mM HEPES, pH 7.9, 25% glycerol, 1.5 mM $MgCl_2$, 0.02 M KCl, 0.2 mM EDTA, 0.2 mM PMSF, 0.5 mM DTT). Release of nuclear proteins was obtained by the addition of a high-salt buffer (as low-salt buffer, but with 1.2 M KCl). Protein concentration was measured according to the

Bradford method. Protein–DNA interactions were analysed by electrophoresis mobility shift assays (EMSAs). End-labelled duplex 5nM dsNHE or 32R-quadruplex were incubated in 20 µl solution containing 20 mM Tris–HCl, pH 8, KCl 30 mM, $MgCl_2$ 1.5 nm, DTT 1 mM, glycerol 8%, Phosphatase Inhibitor Coktail I (Sigma, Milan, Italy) 1%, NaF 5 mM, Na_3VO_4 1 mM, poly [dI-dC] 2.5 ng/µl, nuclear extract 0.25 µg/µl, for 2 h at 37°C. The analyses were carried out in 5% polyacrylamide gels in TBE at 20°C.

Pull-down assays

Ten milligrams of nuclear protein extracts (0.71 mg/ml) were incubated for 2 h with 85 nm biotinylated 32R or duplex NHE in a solution containing Tris–HCl pH 8 20 mM, glycerol 8%, KCl 150 mM, $MgCl_2$ 1.5 mM, poly [dI-dC] 2.5 ng/µl (about two times more concentrated than biotinylated DNA), Na_3VO_4 1 mM, NaF 5 mM, DTT 1 mM, PMSF 0.2 mM. One milligram of Streptavidin MagneSphere Paramagnetic Particles (Promega, Milan, Italy) was added and incubated for 30 min at room temperature. Particles were captured with a magnet and the proteins were eluted with the buffer containing increasing amounts of NaCl (0, 0.1, 0.25, 0.5, 0.75 and 1 M). For further analyses the proteins eluted were concentrated and desalted with Microcon YM-3 filters (Millipore, Billerica, MA).

SDS–PAGE protein analysis

Silver staining. Proteins were separated in 8% SDS–PAGE, the gel was fixed overnight with three changes of 5% acetic acid, 30% ethanol, sensitized in 0.02% $Na_2S_2O_3$ for 1 min, then stained for at least 30 min with 0.026% formaldehyde and 0.4% $AgNO_3$. Development was performed with 3% K_2CO_3 anhydrous, 0.01% formaldehyde and 0.001% $Na_2S_2O_3$. Reaction was stopped with 4% Tris and 2% acetic acid.

Colloidal Coomassie blue staining. Proteins were run on 8% SDS–PAGE, the gel was fixed for 1 h with 45% methanol, 1% acetic acid, then stained overnight with a solution of 1.29 M $(NH_4)_2SO_4$, 0.1% Coomassie G250, 0.5% acetic acid and 34% methanol. Gel was destained with water for a good visualization of the bands that were excised for LC-MS/MS analysis.

Southwestern blots. Twenty-fiive micrograms of nuclear protein extract were loaded in each lane, separated in 8% PAGE–SDS gel and electroblotted in 25 mM Tris, 192 mM glycine, 20% methanol, 0.1% SDS on a nitrocellulose transfer membrane. Denaturation was performed with 6 M guanidine–HCl for 30 min at 4°C, followed by renaturation with increasing dilutions with HEPES binding buffer (25 mM HEPES pH 7.9, 4 mM KCl, 3 mM $MgCl_2$), 1 : 1, 1 : 2, 1 : 4, each wash was carried out at 4°C for 15 min. The blotted membrane was treated for 1 h with 5% non-fat milk in HEPES-binding buffer. Hybridizations with radiolabelled 32R or mutant sequence 32R-4C were carried out in 0.5% non-fat dried milk, 1% NP40, 10 µg/ml poly [dI-dC], in HEPES-binding buffer, 1000 c.p.m./ml of radiolabelled probe, which was preincubated in Tris–HCl 50 mM pH 7.4, KCl 100 mM for 2 h at 37°C. Washes were performed with HEPES-binding buffer.

Protein identification by mass spectrometry

After the separation of proteins by SDS–PAGE, Coomassie-stained protein bands were excised and processed to obtain a tryptic digest as previously described (34). LC-MS/MS analyses were performed on a Micromass CapLC unit interfaced to a Micromass Q-Tof Micro mass spectrometer (Waters, Milan, Italy) equipped with a nanospray source. For each gel spot, 6.4 µl of tryptic digest were injected at a flow rate of 20 µl/min onto an Atlantis dC18 Trap Column. After valve switching, the sample was separated on an Atlantis dC18 NanoEase column ($150 \times 0.075\,mm^2$, 3 µm particle size) at a flow rate of 4.0 µl/min using a gradient from 10% B to 55% B in 27 min (solvent A: 95% H_2O, 5% acetonitrile, 0.1% formic acid; solvent B: 5% H_2O, 95% acetonitrile, 0.1% formic acid). Instrument control, data acquisition and processing were achieved with MassLynx V4.1 software. The MS/MS data were analysed by the online MASCOT software (Matrix Science, http://www.matrixscience.com) against the human section of the MSDB database (release 31 August 2006) (35). The following parameters were used in the MASCOT search: trypsin specificity; maximum number of missed cleavages: 1; fixed modification: carbamidomethyl (Cys); variable modifications: oxidation (Met) and acetyl (N-term); peptide mass tolerance: ±1.0 Da; fragment mass tolerance: ±0.5 Da; protein mass: unrestricted; mass values: monoisotopic. All the identifications were considered reliable if at least two different peptides matched to the protein with significant scores. Only in the case of sample p34, one tryptic peptide was considered enough for the identification because it was associated with the MS/MS spectrum with a high score.

RNA extraction, RT and real-time PCR

Total RNA was extracted from differently treated cells (Panc-1 cells untreated or treated with 50 µM TMPyP2, TMPyP3 or TMPyP4) using Trizol reagent (Invitrogen, Carlsbad, CA), following manufacturer instruction. cDNA synthesis: 5 µl of RNA in diethyl pyrocarbonate (DEPC) treated water (extracted from about 12 500 Panc-1 cells) was heated at 70°C and placed in ice. The solution was added to 7.5 µl of mix, containing (final concentrations) 1× buffer; 0.01 M DTT (Invitrogen); 1.6 µM primer dT [MWG Biotech, Ebersberg, Germany; $d(T)_{16}$]; and 1.6 µM Random primers (Promega); 0.4 mM dNTPs solution containing equimolar amounts of dATP, dCTP, dGTP and dTTP (Euroclone, Pavia, Italy); 0.8 U/µl RNAse OUT; 8 U/µl of M-MLV reverse transcriptase (Invitrogen). The reactions were incubated for 1 h at 37°C and stopped with heating at 95°C for 5 min. As a negative control the reverse transcription reaction was performed with 5 µl of DEPC water. Real-time PCR reactions were performed with 1× iQ™ SYBR Green Supermix (Bio-Rad Laboratories, CA, USA), 300 nm of each primer, 1/10 of RT reaction. The sequences of the primers used for *KRAS* and *GAPDH* amplifications are reported in

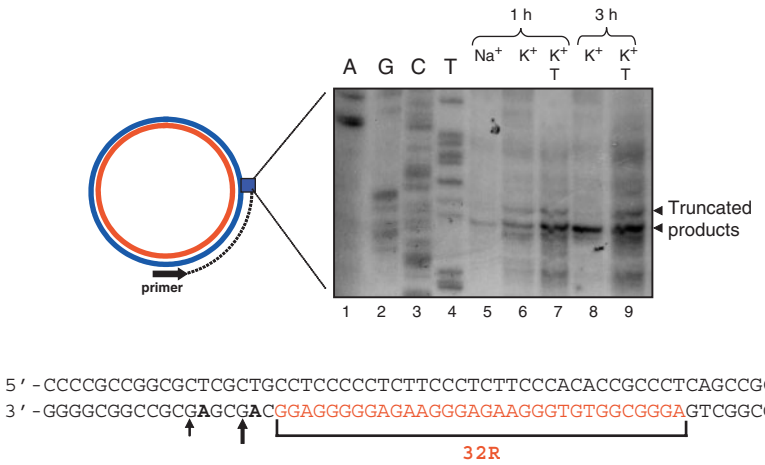

Figure 1. Polymerase stop assay. Lanes 1–4 show sequencing reactions by the dideoxy method. Primer extension reactions were performed in the Klenow buffer, in the presence of 100 mM NaCl (lane 5), 100 mM KCl (lanes 6 and 8), 100 mM KCl plus 100 nM TMPyP4 (T) (lanes 7 and 9). Two DNA polymerase pauses are observed in the presence of KCl plus TMPyP4. The exact positions at which DNA polymerase I is arrested are indicated with arrows. As DNA template for the primer extension reactions we used a plasmid containing *KRAS* NHE. The primer extention reactions have been performed after incubation of the samples for 1 or 3 h at 50°C.

Table 1. The PCR cycle was: 3 min at 95°C, 30 cycles 10 s at 95°C, 30 s at 60°C with an iQ5 real-time PCR controlled by an Optical System software version 2.0.

Cell culture

The human cell line used is from pancreatic adenocarcinoma (Panc-1). The cells were maintained in exponential growth in Dulbecco's modified eagle's medium (DMEM) medium containing 100 U/ml penicillin, 100 mg/ml streptomycin, 20 mM L-glutamine and 10% foetal bovine serum (Euroclone, Pavia, Italy). Cell viability was measured by MTT assays following standard procedures.

RESULTS

The nuclease hypersensitive element of *KRAS* forms quadruplex structures

The promoter of the human *KRAS* gene contains a NHE from −327 to −296, positions relative to the exon φ/intron 1 boundary (16–18) (accession no. L00044). Evidence that this critical promoter element is structurally polymorphic was obtained by primer extension assays, using as template a vector containing NHE. Figure 1 illustrates the results of a typical primer-extension experiment where DNA polymerase is arrested at the 3′end of the G-rich strand of NHE. Considering that this segment contains four runs of guanines and that the arrest of DNA polymerase is potassium-dependent, it is likely that the G-rich strand assumes a G-quadruplex structure. In the presence of NaCl, the pause of DNA polymerase I is weak (lane 5) and a full-length product is observed in the well (data not shown). In contrast, with KCl or KCl + TMPyP4, a cationic porphyrin-stabilizing G4-DNA (36,37), the arrest of DNA polymerase appears stronger, after 1 or 3 h of reaction (lanes 6–9) and a low amount of full-length product is observed in the wells (data not shown). In light of this experiment, we focused on a sequence of 32 bases (32R), comprising fours runs of guanines and located immediately downstream from the DNA polymerase arrests (Figure 1).

To see if 32R assumes a secondary structure we first performed spectroscopic experiments. In 100 mM KCl, but not in 100 mM LiCl, 32R shows a thermal differential spectrum (TDS) typical of quadruplex DNA, with negative bands at 295 and 225 nm, positive bands at 250, 260 and 275 nm (38) (Figure 2a). For comparison we also report the TDS of the *CMYC* sequence (Table 1), which is known to form a parallel G-quadruplex (39). The CD spectrum of 32R is typical of DNA in the parallel quadruplex conformation (40), as it is characterized by a strong and positive ellipticity at 260 nm, which upon denaturing is strongly reduced (from 23 to 8 mdeg) (Figure 2b).

In order to determine the molecularity of the G-quadruplex formed by 32R, we performed native electrophoresis, taking advantage of the fact that oligonucleotides folded into compact G-quadruplex structures migrate faster than oligonucleotides of the same length that are unstructured or self-associated into inter-molecular structures. Figure 2c shows that, in a non-denaturing gel containing 50 mM KCl, 32R migrates faster (band Q_1) than its complementary strand (32Y), a 32-mer unstructured oligonucleotide (32deg) and duplex 32R:32Y (dsNHE). When the concentration of 32R is increased from 20 nm to 1 μM and the sample incubated for 24 h, it still migrates as an intra-molecular G-quadruplex. The addition of five equivalents of TMPyP4 to the samples containing 32R in 50 or 140 mM KCl, gives rise to a new fast-moving species (band Q_2). This suggests that the porphyrin stabilizes a new G-quadruplex conformation that migrates faster than Q_1. The transformation of Q_1 into Q_2 is likely to require an intra-molecular rearrangement. That's why Q_2 is observed after a pre-incubation of 12 h at 37°C, but not at 4°C. As expected, when the PAGE experiment was carried out in 50 or 140 mM LiCl, with and without TMPyP4,

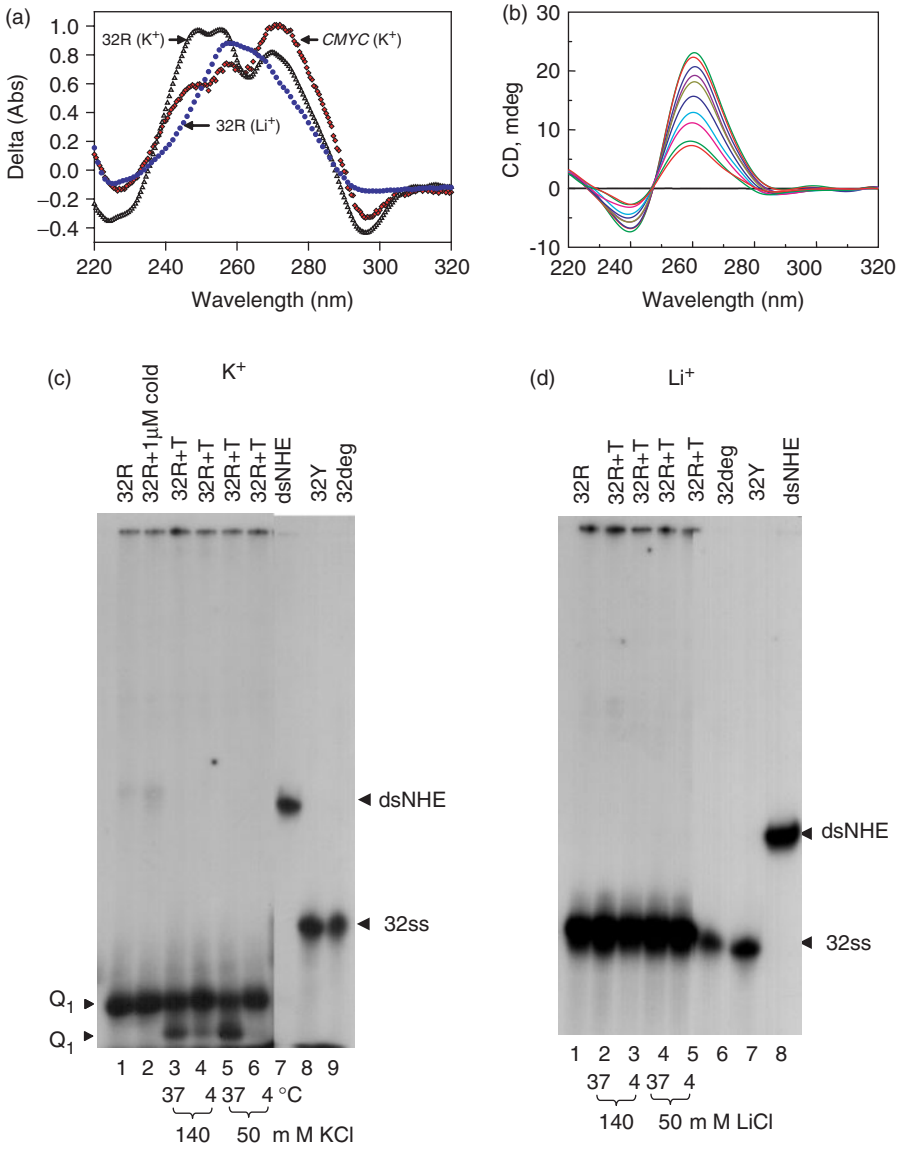

Figure 2. (**a**) Thermal differential spectra of 3 μM 32R (black open triangle) and *CMYC* (red open diamond) (*CMYC* sequence in Table 1) in 50 mM Tris–HCl, pH 7.4, 100 mM KCl. The spectrum of 3 μM 32R (blue filled cirlce) in 50 mM Tris–HCl, pH 7.4, 100 mM LiCl is also shown; (**b**) circular dichroism spectra as a function of temperature of 3 μM 32R in 50 mM Tris–HCl, pH 7.4, 100 mM KCl; spectra from top to bottom have been obtained at 20, 30, 40 50, 60, 65, 70, 75, 80, 90; (**c**) 15% non-denaturing PAGE (TBE 1×, 50 mM KCl in the gel and running buffer) of 20 nM ^{32}P-labelled 32R, dsNHE (32R hybridized to complementary 32Y), 32Y and 32deg (32ss indicates a single-stranded unstructured 32-mer oligonucleotide), incubated overnight in 50 mM Tris–HCl, pH 7.4, 10 mM $MgCl_2$, 140 mM KCl (buffer A) as follows. Lane 1: 32R in buffer A, heated at 95°C just before loading; lane 2: 32R added with cold 32R up to 1 μM in buffer A, heated at 95°C and incubated at 37°C for 24 h before loading; lanes 3 and 4: 32R + 5 eq. TMPyP4 (T) incubated overnight (at 37 or 4°C) in buffer A; lanes 5 and 6: 32R + 5 eq. TMPyP4 (T) incubated overnight (37°C or 4°C) in 50 mM Tris–HCl, pH 7.4, 10 mM $MgCl_2$, 50 mM KCl; lanes 7–9: dsNHE, 32Y and 32deg incubated overnight in buffer A; (**d**) 15% non-denaturing PAGE performed as in (c) but with Li+ instead of K+.

32R migrates as 32Y and 32deg. This indicates that 32R does not form G4-DNA structures in the lithium buffer (Figure 2d).

Fluorescence melting experiments show that two quadruplexes are formed by the G-rich strand of NHE

Tandem repeats of guanines can adopt a variety of intramolecular G-quadruplex structures, each characterized by a definite folding topology. To investigate the folding of the G-rich strand of NHE we used fluorescence spectroscopy and labelled the 5′ and 3′ ends of 32R with FAM and TAMRA, respectively. In LiCl (up to 100 mM), upon excitation at the FAM absorption band (475 nm), a fluorescence emission band is observed at 525 nm due to FAM. As fluorescence emission is not observed at 585 nm (TAMRA), there is no fluorescence resonance energy transfer (FRET) from FAM to TAMRA, in keeping with the fact that in lithium 32R does not form any structure (Figures 2 and 3a). When 32R is in the random-coiled conformation, the two fluorophores are expected to be at a

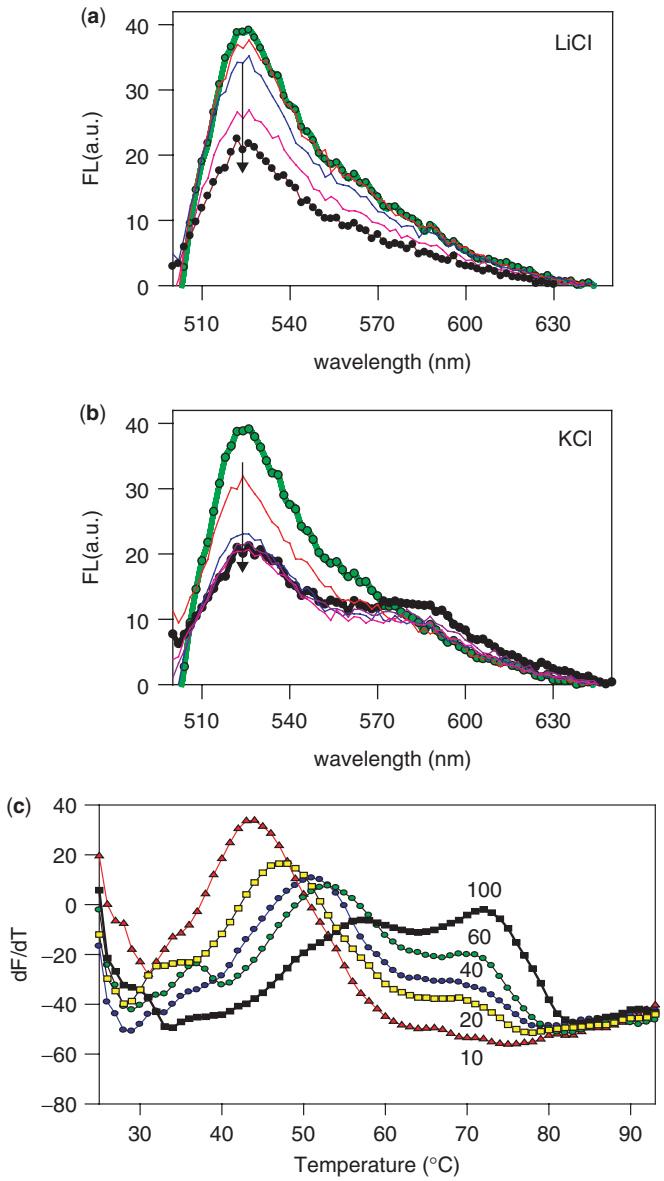

Figure 3. Fluorescence emission spectra (500–650 nm) of 300 nm dual-labelled 32R incubated at 37°C in 50 mM Tris–HCl, pH 7.4, at different LiCl (**a**) or KCl (**b**) concentrations (10, 20, 40, 60 and 100 mM, the arrow indicates the KCl(or LiCl)-increment direction). Excitation wavelength was 475 nm; (**c**) First derivative fluorescence melting curves (dF/dT versus T) of 300 nm dual-labelled 32R in 50 mM Tris–HCl, pH 7.4, at different KCl concentrations (10, 20, 40, 60, 100 mM). Before measurements, the samples were incubated overnight in the appropriate buffer.

distance of about 130 Å, which is higher than the Föster radius (R_o = 45–60 Å) for efficient FRET (41). The quenching effect on FAM observed upon addition of lithium is probably due to the guanines nearby to the fluorophores (42). Replacing lithium with potassium, the fluorescence emission spectrum of the dual-labelled 32R sequence shows bands at both 525 and 585 nm (Figure 3b). This indicates that potassium induces the folding of 32R into a G-quadruplex structure in which the two dyes come within the Föster distance. Two observations can be made.

Table 2. Thermal stability of the G-quadruplexes Q_1 and Q_2 of the G-rich strand 32R of the *KRAS* promoter in 50 mM Tris–HCl, pH 7.4, KCl as indicated in column 1

KCl (mM)	Q_1 (°C)[a]	Q_2 (°C)[a]
10	44	–
20	48	69.5
40	51	70.0
60	53	71.0
100	55	72.0

[a]Value uncertainty is ±1°C.

First, the fluorescence intensity of FAM decreases when potassium is increased, because of the energy transfer from FAM to TAMRA, due to quadruplex formation. Second, TAMRA emission increases with potassium. This is evident if one measures the intensity ratio F_{585}/F_{525}: it increases from 0.24 to 0.58 in 0–100 mM KCl, while it remains constant at ~0.24 in 0–100 mM LiCl. It has been suggested that the modest increase of TAMRA, which is generally observed, might be due to a decrease in molar absorptivity of the molecule and/or to a static quenching caused by interactions with the FAM moiety (43). Excitation spectra monitored at wavelength of TAMRA emission (585 nm) showed two bands that corresponded to TAMRA and FAM absorption maxima, supporting the presence of FRET when 32R is exposed to potassium (data not shown). To determine the stability of the G-quadruplex we performed fluorescence melting experiments as previously described (44,45). Basically, upon fluorescein excitation at 475 nm one observes an increase in the emission at 525 nm between the low-temperature (folded/quenched) and high-temperature (unfolded/bright fluorescent) form. Figure 3c shows the first derivative of the fluorescence (dF/dT) versus T for dual-labelled 32R, after incubation in the buffer added with increasing amounts of KCl. Two clear transitions are observed in the KCl concentration range of 20–100 mM (at 10 mM KCl only one transition is observed). The T_m of these transitions are reported in Table 2. The first transition occurs in the temperature range of 44–55°C, while the second occurs in the range of 67–72°C. As these transitions are only observed in the presence of potassium ions, they are due to the melting of two distinct G-quadruplex structures. On the other hand, the existence of two-folded conformations for 32R is not only suggested by the melting experiments but also by gel electrophoresis. Figure 2c showed that in the presence of five equivalents of TMPyP4, 32R migrates, after incubation at 37°C, with two-folded fast-running compact conformations (Q_1 and Q_2). As TMPyP4 promotes the transformation of Q_1 into Q_2, we investigated the melting of 32R in the presence of TMPyP4. Figure 4a shows the melting curves of 32R in Tris-buffer containing 100 mM KCl and different amounts of TMPyP4 (TMPyP4/32R ratios of 0, 1, 3 and 5). In 100 mM KCl, 32R shows the typical biphasic profile due to the melting of quadruplexes Q_1 and Q_2, as previously observed. The addition of TMPyP4 induces the transformation of Q_1 into Q_2. At the TMPyP4/32R ratios of 3 or 5, 32R shows a monophasic

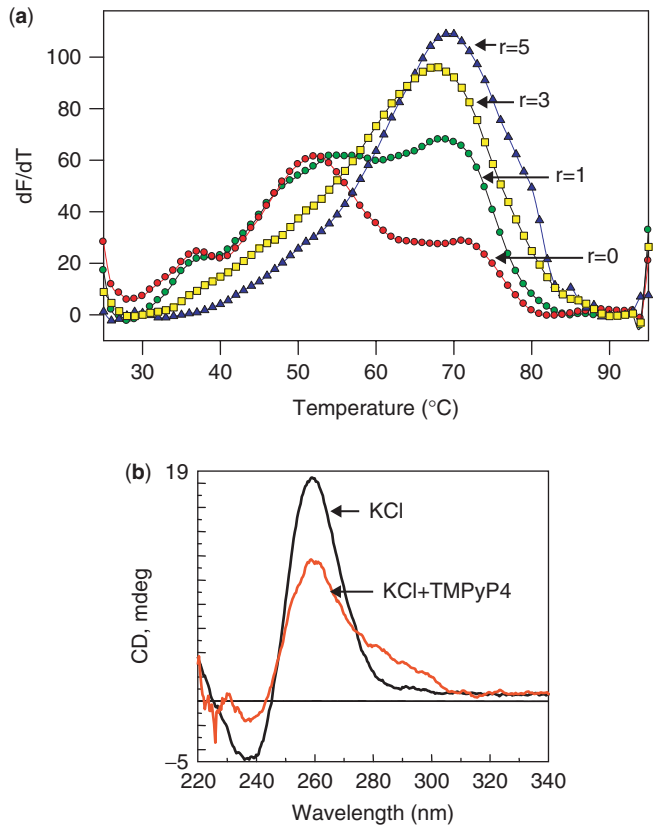

Figure 4. (**a**) dF/dT *versus* T melting curves of 300 nM dual-labelled 32R in 50 mM Tris–HCl, pH 7.4, 100 mM KCl at TMPyP4/32R ratios (r) of 0, 1, 3 and 5; (**b**) CD spectra of 32R in 50 mM Tris–HCl, pH 7.4, 100 mM KCl, room temperature, in the presence and absence of 5 eq. of TMPyP4. The oligonucleotide concentration was 3 μM, pathlength cell 0.5 cm, ellipticity expressed in millidegrees.

denaturing curve with a T_m ~72°C (Q_2). In conclusion, FRET data shows that the polypurine strand of NHE can potentially adopt one of the two possible G-quadruplex conformations, which are inter-convertible by increasing the temperature and/or adding TMPyP4.

It is interesting to observe that the CD of 32R in 100 mM KCl changes upon addition of five equivalents of TMPyP4, the intensity of the 260 nm ellipticity is reduced and a new positive ellipticity at 295 nm is generated (Figure 4b). This might suggest that the folding topology of quadruplex 32R changes from a parallel (46) to a mixed parallel/anti-parallel quadruplex (47). This finding is in accordance with previous data showing that, upon binding, TMPyP4 and Se2SAP promote the conversion of the G-quadruplex of *CMYC* from the parallel to the mixed parallel/anti-parallel conformation (48,49).

G-quadruplex structure of 32R: DMS footprinting and CD studies

To gain an insight in the folding of 32R we used chemical footprinting with DMS. After overnight incubation in 100 mM LiCl, 37°C, 32R does not show any footprinting (lane 2 and Figure 5a), suggesting that the sequence does not form any secondary structure, in accordance with

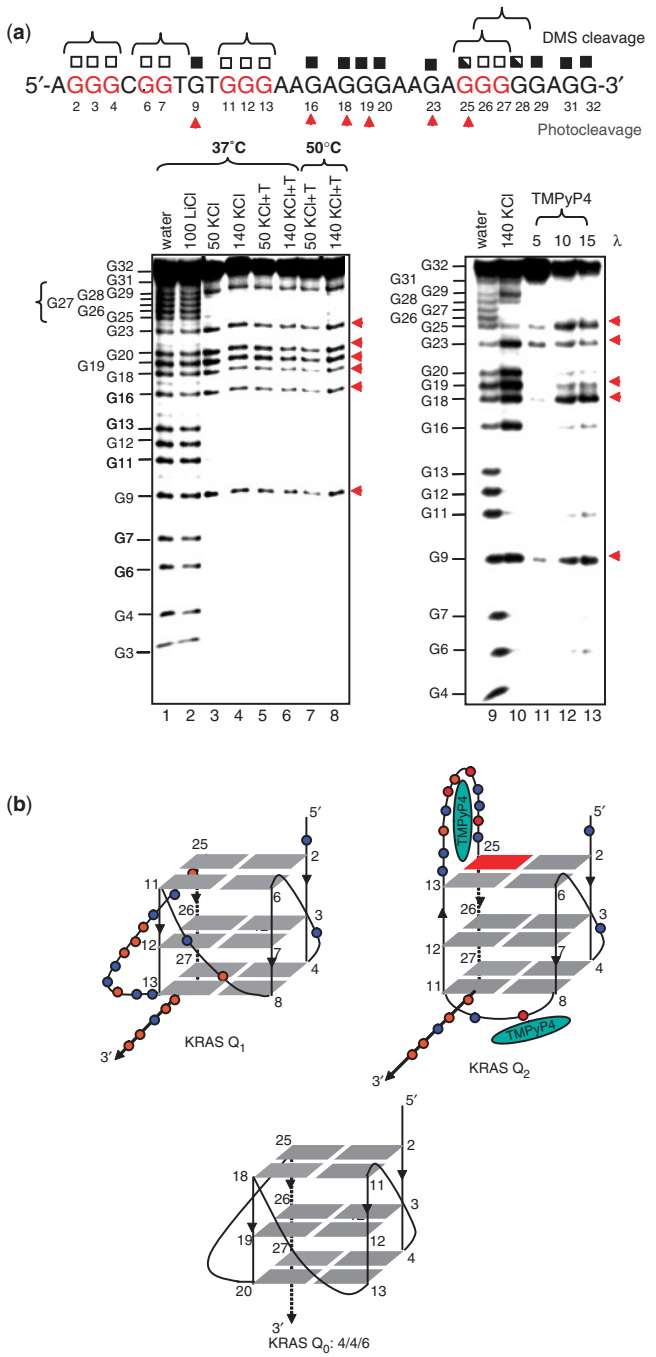

Figure 5. (**a**, left) DMS-footprinting of 32R at 37°C in 50 mM sodium cacodylate, pH 8, 1 mM EDTA 1 μg sonicated salmon sperm DNA (buffer B). 32R incubated overnight in water (lane 1); 32R incubated overnight in buffer B plus 100 mM LiCl (lane 2); 32R incubated in buffer B plus 50 or 140 mM KCl, 37°C, (lanes 3 and 4); 32R incubated in buffer B plus 50 or 140 mM KCl + 5 eq. TMPyP4 (lanes 5 and 6); 32R in buffer B plus 50 or 140 mM KCl, 50°C, (lanes 7 and 8); (**a**, right) 32R in buffer B plus 140 nM KCl (lane 10); 32R incubated overnight in buffer B, 100 mM KCl and 5 eq. of TMPyP4, irradiated for 5, 10 and 15 min (lanes 11–13);.(**b**) The proposed G-quadruplex structures for 32R inferred from footprinting studies. The circles in Q_1 and Q_2 indicate the bases of the loops: red, guanine; blue, A or T or C. Guanine 25 in Q_2 is shown in red to indicate that is strongly photocleaved by TMPyP4. The expected quadruplex Q_o is not supported by DMS-footprinting. The symbols above the sequence at the top mean: cleaved base (full square); uncleaved base (open square); partially cleaved base (semi-full square).

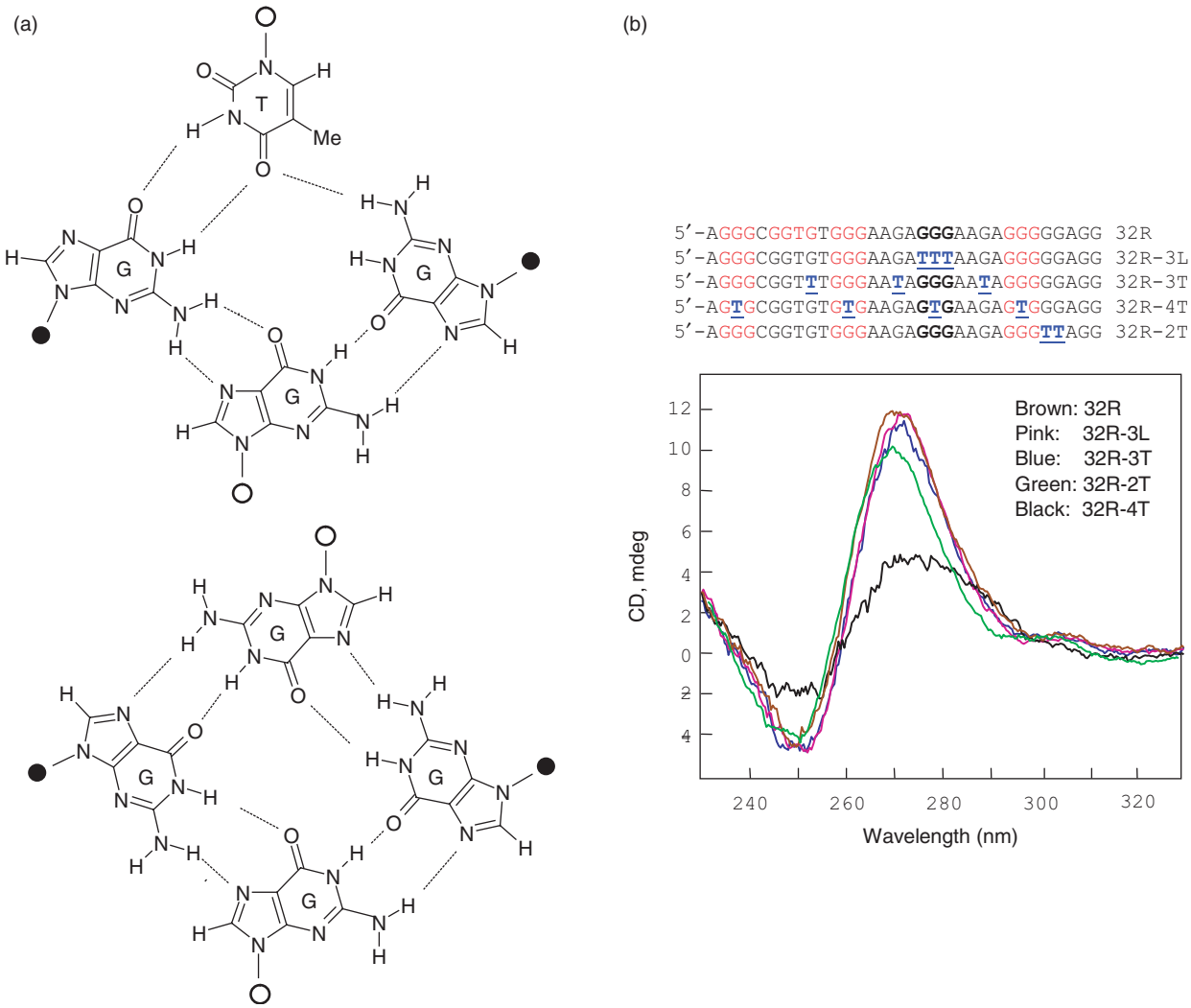

Figure 6. (**a**) Structures of the putative GGGT and GGGG tetrads; (**b**) CD spectra of 32R mutant sequences in 50 mM Tris–HCl, pH 7.4, 100 mM KCl. Oligonucleotide concentration was 3 μM, pathlength cell 0.5 cm, ellipticity expressed in millidegrees.

FRET and PAGE data. However, in 100 mM KCl, 37°C, 32R shows a clear and reproducible footprinting where 11 guanines out of 21 appear protected from DMS/piperidine cleavage (G2 is not seen in the gel). Although 32R contains four runs of guanines that could allow a straightforward fold into a parallel quadruplex with two external loops of 4 bases and one of 6 bases (Figure 5b, Q_0), the footprinting data indicate that 32R folds into a G-quadruplex with a different folding topology. This is indicated by the fact that the central run of guanines G18–G20 is cleaved and the couple of guanines G6–G7 is protected from cleavage under a variety of conditions: 37°C or 50°C, 50 or 140 mM KCl, with or without 5 eq. of TMPyP4 (Figure 5a and lanes 3–8). Since 32R does not fold into a hairpin (this structure should have also been observed in Li-buffer), its DMS-footprinting, which is highly reproducible, is consistent with the formation of a parallel G-quadruplex with external loops of 1, 2 and 11 bases (Figure 5b, quadruplex Q_1). Quadruplex Q_1 is likely to have thymidine T8 directly involved in the formation of the G-tetrad core. On the other hand, mixed guanine/thymine tetrads have been previously observed by NMR and the structure of the putative GGGT tetrad is derived from that reported for GTGT (50) (Figure 6a). It is worth noting that thymidine has been reported to also form TTTT (51) and ATAT (52) tetrads. Compared to a canonical G-tetrad that is stabilized by eight hydrogen bonds, GGGT has one less H-bond. Alternatively, one cannot exclude that guanine G9 is involved in the formation of the G-tetrad. In this case, the run of guanines G6–G9 should contain T8 as a flipped-out base and the resulting G-quadruplex should have two one-base double-chain reversal loops. This possibility, however, is not supported by the fact that G9 is reactive to DMS. One could argue that T8, being an intervening base between G7 and G9, might cause a backbone distortion in the neighbourhood of G9, which weakens the hydrogen bond involving N7 of G9. Another aspect that is worth noting is that a close inspection of the autoradiographies showed that G25 and G28 appear always partially protected (lane 10). This may result from the fact that two loop isomers of Q_1 may exist in solution: one involving the run

of guanines G25-G26-G27, the other the run G26-G27-G28. The preference of forming Q_1 with 1/1/11 or 1/2/11 loops instead of Q_0 with 4/4/6 loops can be rationalized by the finding that single-nucleotide loops stabilize quadruplex DNA more than larger loops (53).

To obtain further evidence that 32R in 100 mM KCl folds into Q_1, we analysed the CD of a number of 32R mutant sequences (Figure 6b). It can be seen that: (i) when the run of guanines G18–G20, which is supposed to be part of the 11-base loop, is replaced with T's (mutant 32R-3L), the CD does not change; (ii) when G9, G16 and G23, which should be located in the external loops, are replaced with T's (32R-3T), the CD does not change either; (iii) when G28 and G29, located in the penta-guanine stretch near the 3′ end of the sequence, are replaced with T's (32R-2T), the CD does not appreciably change; (iv) when G2, G12, G19 and G26, bases located in the runs of guanines (32R-4T), are replaced with T's, the 260-nm ellipticity is dramatically reduced, indicating that the mutant does not assume any secondary structure. Together, these CD spectra support the structure assigned to Q_1.

As shown by fluorescence-melting and PAGE, 32R in the presence of TMPyP4 adopts a more stable quadruplex conformation with $T_m = 72°C$ (Q_2). The CD of 32R obtained in the presence of TMPyP4 suggests that Q_2 should have a structure with both parallel (260 nm ellipticity) and anti-parallel (295 nm ellipticity) characters. We propose for Q_2 a mixed parallel/anti-parallel topology with one-base double-chain reversal loop and two lateral loops of 2 and 11 bases (Figure 5b). Since TMPyP4 is a porphyrin that upon irradiation generates reactive oxygen species that cleave DNA in the neighbourhood of the binding site, we performed photocleavage experiments with 32R. We observed that the bases that are strongly photocleaved are located in the lateral 11-base (G18, G19 and G23) and 2-base (G9) loops (Figure 5a, lanes 11–13). This is consistent with the finding that the porphyrin preferentially binds to the loops of intramolecular quadruplexes (54). But, the fact that G25 and slightly also G11 and G6 are photocleaved supports the notion that TMPyP4 binds also to the external G-tetrads (36,37). This photocleavage pattern is substantially in accordance with the folding proposed for quadruplex Q_2.

The binding of nuclear proteins to duplex NHE is competed by 32R in the G-quadruplex form

NHE is a regulatory element of the *KRAS* promoter that is essential for transcription (16–18). When dsNHE is incubated with a pancreatic adenocarcinoma (Panc-1) nuclear extract, three DNA–protein complexes, namely C1, C2 and C3, are observed by EMSA (Figure 7a,

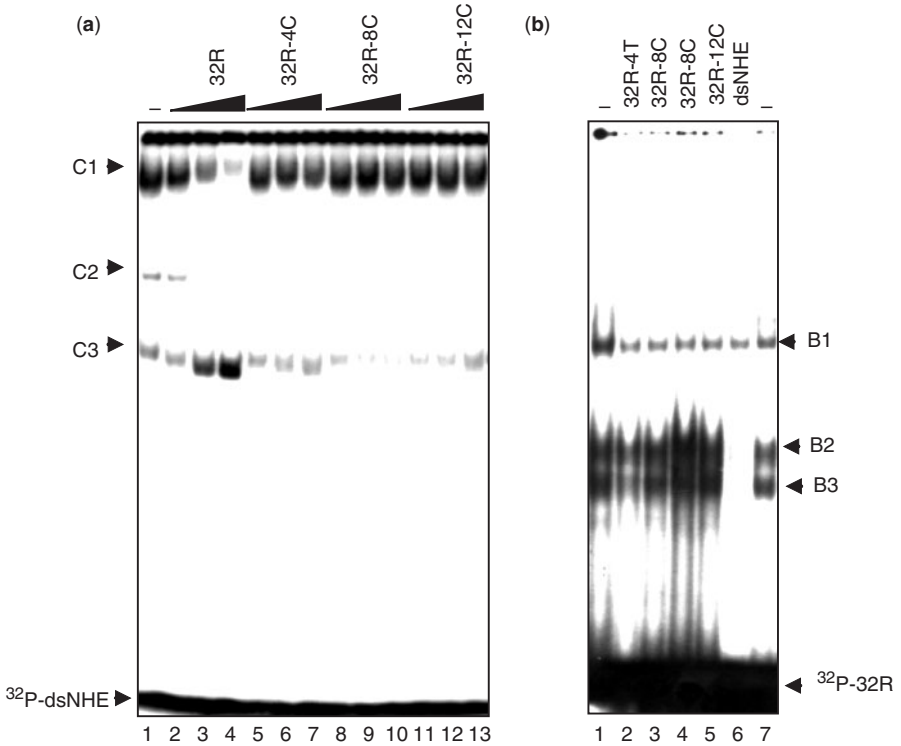

Figure 7. Competition binding experiments. When ^{32}P-labelled dsNHE is incubated for 2 h at 37°C with a nuclear protein extract from Panc-1 cells, two main DNA–protein complexes (C1 and C3) are observed in a 5% PAGE in TBE at room temperature (**a**) The formation of the DNA–protein complex C1 is competed by 32R, but not by its mutant sequences 32R-4C, 32R-8C and 32R-12C (their sequences are in Table 1), that are unable to assume a G-quadruplex conformation, added to the reaction mixtures in excess over duplex dsNHE. Lanes 2–4: radiolabelled dsNHE (5 nM), 2 μg extract, 32R (competitor) 10-, 50-, 100-fold in excess respect dsNHE, respectively; lanes 5–7: same loading but with 32R-4C as competitor; lanes 8–10: same loading but with 32R-8C as competitor; lanes 11–13: same loading but with 32R-12C as competitor (**b**) When ^{32}P-labelled 32R is incubated for 2 h at 37°C with the Panc-1 nuclear extract, three major DNA–protein complexes, B1, B2 and B3 are observed by 5% PAGE. The DNA–protein complex B1 is partially competed by the mutant oligonucleotides 32R-4T (30×, lane 2), 32R-8C (20× and 30×, lanes 3 and4), 32R-12C (30× lane 5), dsNHE (30×, lane 7). Complexes B2 and B3 are not competed by the mutant oligonucleotides, but they are competed by dsNHE.

lane 1). In order to see if the proteins that bind to dsNHE also recognize the G-rich strand (32R), folded in its G-quadruplex conformation, we performed competition experiments. We found that 32R competed efficiently the DNA–protein complex C1. The addition of 50-fold excess of 32R inhibits the formation of complex C1 by >50%, 100-fold excess practically abrogates complex C1. In contrast, mutant sequences 32R-4C, 32R-8C and 32R-12C (Table 1), which do not fold into a quadruplex structure (according to CD), did not affect the formation of C1 at all, suggesting that 32R competes with dsNHE for protein binding through its secondary structure. It is interesting to note that the competition of C1 results in an increase of C3, suggesting that C3 is probably a partially assembled form of the DNA–protein complex C1. We also observed that complex C1 is competed, though less efficiently than 32R, by the *CMYC* quadruplex-forming sequence (Table 1), which is known to form a parallel quadruplex (39), but it is not competed by the pyrimidine strand of NHE (32Y)(Supplementary Data S1). Direct evidence that the G-quadruplex formed by 32R binds to proteins from Panc-1 nuclear extract was obtained by EMSA (Figure 7b). Radiolabelled 32R, pre-equilibrated in 100 mM KCl and successively incubated with the nuclear extract for 30 min, formed three distinct DNA–protein complexes (B1, B2 and B3). As complex B1 is partially competed by mutants 32R-4T, 32R-8C, 32R-12C (Table 1) and dsNHE, it is due to a protein binding non-specifically to DNA. Complexes B2 and B3 are not competed by the mutant sequences, but are strongly competed by dsNHE. This suggests that B1 and B2 contain proteins that recognize both quadruplex and double-stranded conformations of NHE.

Identification of nuclear proteins binding to the G-rich strand of NHE

We used streptavidin–biotin paramagnetic beads to pull down from Panc-1 nuclear extract the proteins binding to dsNHE under physiological conditions: in 20 mM Tris–HCl pH 8, 1.5 mM $MgCl_2$, 2.5 ng/µl poly [dI-dC], 150 mM KCl, 37°C. After binding, the proteins were eluted from the beads in three steps with Tris-buffers containing increasing concentrations of NaCl (0.25, 0.5 and 0.75 M). The fractions obtained were desalted and analysed by SDS–PAGE/silver staining. Three polypeptides co-eluted in the high salt fraction: p114, p86 and p70 (Figure 8a, lanes 5–7). In parallel, the nuclear extract was applied to magnetic beads coupled to 32R in the G-quadruplex conformation. Again, the bound proteins were eluted in three steps and the fractions analysed by SDS–PAGE (lanes 2–4). In this case, the polypeptides co-eluting in the high salt fraction are p114, p70 and p34. When the pulled down experiment was performed with the beads coupled with a scramble oligonucleotide (B-scram, Table 1), these specific bands in SDS–PAGE were not obtained (data not shown). The bands were excised from the gel and the proteins identified by mass spectrometry were poly [ADP-ribose] polymerase 1 (PARP-1), ATP-dependent DNA helicase 2, subunit 1 (Ku70) and subunit 2 (Ku86) and heterogeneous nuclear ribonucleoprotein A1 (hnRNP A1) (Supplementary Data S2). The band of p34 contained in addition to hnRNP A1, some isoforms of histone H1. Histone proteins (~20 kDa) are highly basic (pI>10) and they probably interact with NHE by unspecific electrostatic interactions. The predicted molecular masses of proteins identified (113, 86, 70 and 34 kDa) are in nice accord with apparent molecular masses observed by SDS–PAGE (Supplementary Data, S2). The data indicate that

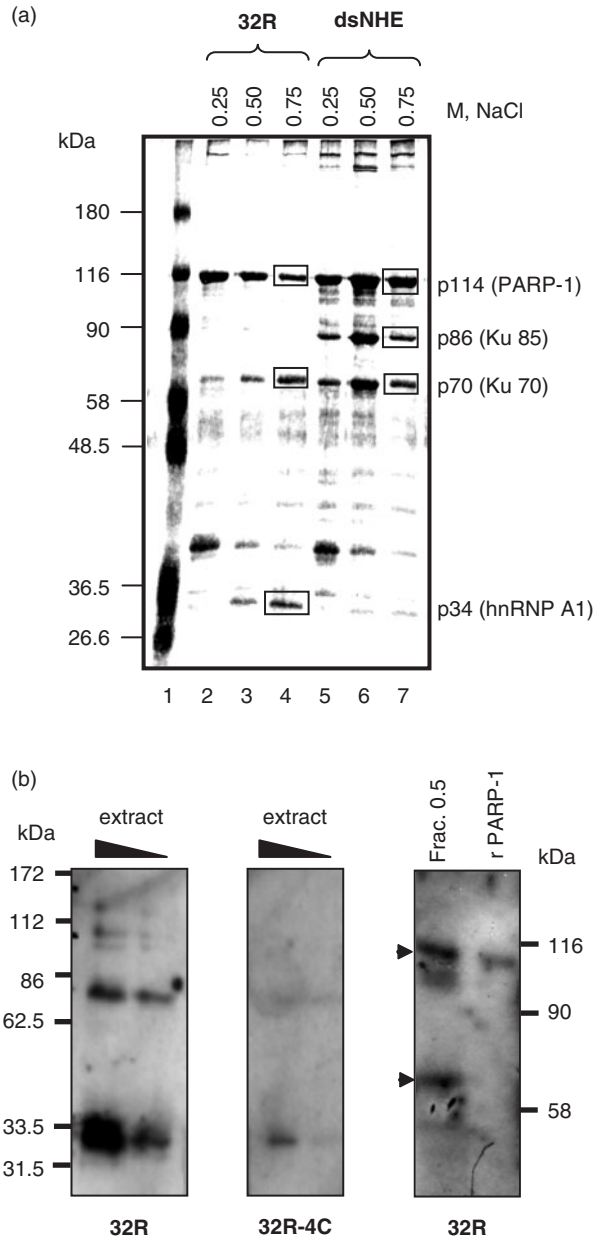

Figure 8. (**a**) SDS–PAGE/silver staining of protein fractions eluted from streptavidin–biotin paramagnetic beads coupled to dsNHE (lanes 5–7) or to quadruplex 32R (lanes 2–4). Bands in the boxes have been excised and subjected to mass spectrometry analysis; (**b**, left) Southwestern blot showing that radiolabelled 32R-quadruplex, but not mutant 32R-4C, recognizes 34 and 70 kDa proteins (hnRNP A1 and Ku70) present in the extract; (**b**, right) Southwestern blot showing that radiolabelled 32R recognizes bands at 114 and 70 kDa (PARP-1 and Ku70) present in the 0.75 M NaCl pull-down fraction (lane 4); as a control it is shown that 32R recognizes recombinant PARP-1 (rPARP-1).

two proteins associated with NHE of *KRAS* (PARP-1 and Ku70) have affinity for both the folded and duplex conformation of regulatory NHE and may provide a rationale for the competition experiments illustrated in Figure 8. It is worth noting that the three proteins binding to quadruplex 32R have been previously found to recognize unusual DNA structures (see Discussion section). The protein that is likely to have an important function in the regulation of *KRAS* transcription is hnRNP A1, as it possesses unfolding capacity against G4-DNA (55). The binding of these proteins to quadruplex 32R was also observed by Southwestern blots. The nuclear extract was run on SDS–PAGE, electroblotted onto nitrocellulose and the proteins renatured in HEPES buffer (see Materials and methods section). The membrane was treated with radiolabelled 32R or 32R-4C (separate experiments). As expected, 32R but not mutant 32R-4C recognized bands at ~34 and 70 kDa (hnRNP A1, Ku70). As for PARP-1, its binding to 32R was difficult to detect, probably because this large protein did not completely renature after SDS–PAGE. However, when the 0.75 M NaCl fraction of the pull-down was electroblotted (lane 4 of Figure 8a) a clear band around 113 kDa was obtained, as expected. As a control, we used recombinant PARP-1 (rPARP-1).

Effect of cationic porphyrins (TMPyP2, TMPyP3 and TMPyP4) on *KRAS* transcription

Considering that the G-rich sequence of NHE can form stable G-quadruplex structures, we asked if these unusual DNA structures have any effect on transcription of genomic *KRAS* in pancreatic adenocarcinoma cells. To this purpose we treated Panc-1 cells with cationic porphyrins that are known to stabilize G4-DNA: TMPyP3 (more specific for parallel inter-molecular quadruplexes) and TMPyP4 (more specific for folded quadruplexes) (56). As a control molecule of interest, we used TMPyP2, a positional isomer (ortho) of TMPyP4 that has very low affinity for G4-DNA (see the structures in Figure 9). The cells (50 000/well, 24-well plate) were treated with 50 μM TMPyP4, total RNA was extracted after 12 and 24 h of incubation. The levels of *KRAS* and *GAPDH* mRNAs were measured by real-time PCR (the primer sequences used are reported in Table 1). The levels of *KRAS* mRNA compared to *GAPDH* mRNA in untreated and treated Panc-1 cells are shown in Figure 9. It can be seen that TMPyP4 induces a significant reduction of *KRAS* mRNA of about 30 ± 4%, at either 12 or 24 h of incubation of the cells with the porphyrin. TMPyP3 slightly inhibits transcription only after 24 h of treatment, while TMPyP2 did not show any effect on the levels of mRNA at both 12 and 24 h, as it is to be expected (56). Our finding that TMPyP4 behaves as a transcription repressor is in keeping with previous results (21–23). We found that TMPyP4 strongly inhibited (~80%) the activity of the murine *KRAS* promoter in a cell line transfected with the porphyrin and a plasmid containing the CAT gene driven by the murine *KRAS* promoter (23). Furthermore, in a recent work Hurley and co-workers reported that 10 μM TMPyP4 inhibited by 50% the transcription of firefly luciferase driven by PDGF-A promoter (27). Here, the effect of

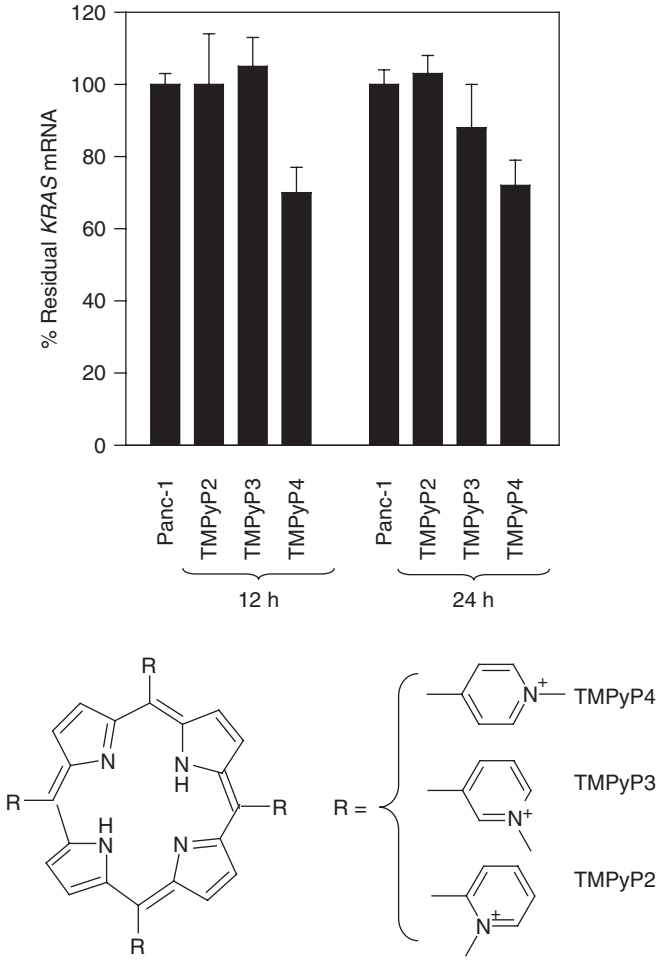

Figure 9. Real-time PCR determination of the level of endogenous *KRAS* mRNA in Panc-1 cells untreated or treated for 12 and 24 h with 50 μM of TMPyP2, TMPyP3 and TMPyP4. The ordinate reports the percent residual *KRAS* mRNA [T/C^*100, where T is (*RAS* mRNA/*GAPDH* mRNA) in treated cells and C is (*RAS* mRNA/*GAPDH* mRNA) in untreated cells]. The structures of the three positional isomers TMPyP2, TMPyP3 and TMPyP4, in which the *N*-methyl group on the pyridyl ring is either in the ortho or meta or para positions, relative to its connection to the porphine core, are shown.

TMPyP4 on human *KRAS* transcription is evaluated at genomic level; the repression reported is lower probably because the porphyrins do not localize efficiently into the nucleus of the cells (57). Finally, the fact that TMPyP2, the porphyrin that cannot stabilize G4-DNA, does not reduce *KRAS* mRNA, suggests that the bioactivity of TMPyP4 is due to specific binding to the G-quadruplex extruded by the regulatory element and not to a non-specific strand breakage.

DISCUSSION

In this study, we demonstrate that a nuclease hypersensitive element of the *KRAS* promoter, located upstream of the major transcription initiation site, is structurally polymorphic. Primer-extension experiments showed that potassium and TMPyP4 induce the arrest of DNA polymerase I

at the 3′ end of the G-rich strand of NHE: a behaviour associated with the formation of an intra-molecular G-quadruplex. Folded quadruplex structures have been found in the promoters/enhancers of a number of genes including murine *KRAS* (23), *CMYC* (21,22), *BCL-2* (24), *VEGF* (26), c-*KIT* (28), PDGF-A (27), hypoxia-inducible factor 1-α (25) muscle-specific human sarcomeric mitochondrial creatine kinase (sMtCK), mouse MCK and α7 integrin genes (29). The G-quadruplex formed by the human *KRAS* sequence has been characterized by non-denaturing gel electrophoresis, CD, UV and FRET spectroscopic data as well as chemical probing with DMS and TMPyP4. We used FRET to analyse the melting of the G-rich strand of NHE (32R), under a variety of ionic strength conditions. In 100 mM KCl, 32R exhibits two transitions with T_m of ~55°C and ~72°C. Since these transitions are not observed in 100 mM LiCl, they have been associated with the melting of two distinct G-quadruplex structures, namely Q_1 and Q_2. When TMPyP4, a cationic porphyrin that stabilizes quadruplex DNA, is added to the K^+-buffer, the transition at 55°C is abrogated, indicating that the ligand induces the transformation of Q_1 into Q_2. Taken together, PAGE and melting data suggest that the G-rich strand of NHE is characterized by the following equilibria:

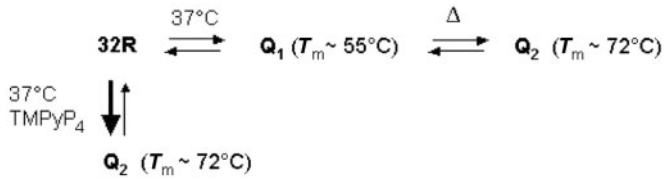

At 37°C, 100 mM KCl, 32R folds into Q_1: a parallel intra-molecular G-quadruplex with T_m ~55°C. Increasing the temperature, Q_1 is disrupted and 32R folds into a new quadruplex (Q_2) with T_m of ~72°C. If TMPyP4 is added to K^+-buffer, 32R can fold into Q_2 even at 37°C, as demonstrated by native electrophoresis, which shows that 32R, after incubation at 37°C in 100 mM KCl + 5 eq. of TMPyP4, migrates with two compact fast running quadruplexes. To propose a structure for Q_1 and Q_2 we performed DMS-footprinting experiments. In the presence of KCl or KCl + TMPyP4, the run of guanines G18–G20 is found to be reactive to DMS, suggesting that the expected quadruplex Q_0 with loops of 4 and 6 bases is not formed (Figure 5b). One could argue that the cleavage pattern reflects the formation of a hairpin, but this can be ruled out because 32R, after incubation in Li^+-buffer, does not show any footprinting and migrates as an unstructured 32-mer oligonucleotide. On the basis of CD and footprinting data we propose for Q_1 a parallel quadruplex with three G-tetrads, three external loops of 1, 2 and 11 bases as well as a G-tetrad involving one thymidine (T8). Figure 6b shows that in this putative G-tetrad NH(3) and O(4) of thymine form hydrogen bonds with O(6), NH(1) and NH2(2) of adjacent guanines, as indicated by NMR data (50). Q_1 fits to the DMS-footprinting data much better than a previous structure that we tentatively assigned to 32R (23). For quadruplex Q_2 we propose a mixed parallel/anti-parallel structure (46,47). The conformation showed in Figure 5b has two lateral and one double-chain reversal loops; but for Q_2 we can also hypothesize a folding topology with one lateral, one diagonal and one double-chain reversal loop (Supplementary Data S4). However, although these structures are in keeping with the experimental DMS-cleavage patterns, they are only hypothetical and need to be confirmed by NMR data.

The formation of G-quadruplexes within a regulatory element of *KRAS* (16–18), suggests that they are likely to play a functional role in transcription. To support this hypothesis, we searched for proteins binding to NHE. To pull-down from a pancreatic adenocarcinoma nuclear extract proteins with affinity to quadruplex DNA, we used streptavidin paramagnetic beads coupled to 32R in the quadruplex form. Three proteins were isolated and identified by mass spectrometry: PARP-1, Ku70 and hnRNPA1. Two of these proteins, PARP-1 and Ku70 (as a dimer with the Ku83 subunit), were found to bind to dsNHE. It is interesting to note that the proteins that bind NHE had been previously implicated in transcription regulation. PARP-1 is known to be part of the excision repair process, but growing evidence indicates that it is also an important component of promoter/enhancer regulatory complexes (58). For instance, PARP-1 specifically binds to a G-rich element of the *REG* gene promoter, forming with other proteins the active transcriptional DNA–protein complex (59). As PARP-1 was reported to recognize DNA hairpins and cruciforms, it could recognize the loop bases of quadruplex 32R (60,61). Ku proteins are highly conserved in eukaryotes and involved in DNA repair, maintenance of telomere length and transcription regulation (62,63). Ku proteins have the capacity to interact with circular DNA with bubbles and any structure containing a double-to-single strand transition (64). *In vitro* data indicate that Ku70 binds to and stabilize the tetrahelical form of the Fragile X syndrome $d(CGG)_n$ expanded sequence (65). However, the protein associated with NHE, which is particularly interesting in the context of *KRAS* transcription is hnRNP A1, as its N-terminus proteolitic portion (residues 1–195), referred to UP1, shows the ability to resolve G4-DNA. Recombinant UP1 has been demonstrated to have G-tetrad destabilizing activity against intra-molecular G-quadruplexes formed by the minisatellite (MN)Pc-1 tandem repeat $d(GGCAG)_5$ (55) and by the telomeric $d(TAGGGT)_4$ repeat (66). It is not yet known how hnRNP A1 and UP1 resolve G4 DNA, but like the proteins active at the telomeres, UP1 should trap single-stranded DNA and shift the single-stranded ⇔ quadruplex equilibrium away from the quadruplex (54). As hnRNP A1 and PARP-1 have been reported to interact with each other, it could be that PARP-1 rybosylates hnRNP A1 and modifies the functional properties of the protein in the context of gene regulation (67).

In the light of these data, we asked how a folded secondary structure formed within NHE might be involved in transcription regulation. The *KRAS* promoter at NHE may undergo, in the presence of superhelical stress, a duplex-to-quadruplex equilibrium. When NHE is in the folded G-quadruplex form, transcription should be inhibited, in accordance with the fact that the stabilization of this structure by TMPyP4 results in a transcription

repression (21,23,27). It is possible that the G-quadruplex of NHE is stabilized by Ku70 (65). The complementary unpaired pyrimidine strand of NHE should be bound by single-stranded binding protein hnRNP K (68). To activate transcription, the G-quadruplex of NHE should be unfolded and this could involve hnRNP A1, because of its capacity to resolve intra-molecular G4-DNA (55,66). Once the promoter assumes a double-stranded conformation, a transcriptional active DNA–protein complex is rapidly assembled. In this scenario, G-quadruplex DNA behaves as a transcription repressor. The model proposed for the control of *KRAS* transcription suggests several strategies to down-regulate *KRAS* in tumour tissues: (i) use of planar macrocycles capable to stabilize G4-DNA and lock the promoter into the folded non-active form (69); (ii) use of triplex-forming oligonucleotides to block the formation of DNA–protein complexes at NHE (70); (iii) use of decoy oligonucleotides against proteins binding to NHE (hnRNP A1/Ku70/PARP-1 and others).

SUPPLEMENTARY DATA

Supplementary Data are available at NAR Online.

ACKNOWLEDGEMENTS

This study has been carried out with the financial support of the Italian Ministry of Education (PRIN 2005) and the Italian Association for Cancer Research (AIRC 2007). Funding to pay the Open Access publication charges for this article was provided by AIRC.

Conflict of interest statement. None declared.

REFERENCES

1. Barbacid,M. (1987) Ras genes. *Annu. Rev. Biochem.*, **56**, 779–827.
2. Malumbres,M. and Barbacid,M. (2003) RAS oncogenes: the first 30 years. *Nat. Rev. Cancer*, **3**, 459–465.
3. Yanes,L., Groffen,J. and Valenzuela,D.M. (1987) cKRAS mutations in human carcinomas occur preferentially in codon 12. *Oncogene*, **1**, 315–318.
4. Nagata,Y., Abe,M., Kobayashi,K., Yoshida,K., Ishibashi,T., Naoe,T., Nakayama,E. and Shiku,H. (1990) Glycine to aspartic acid mutations at codon 13 of the c-Ki-ras gene in human gastrointestinal cancers. *Cancer Res.*, **50**, 480–482.
5. Adjei,A.A. (2002) Blocking oncogenic Ras signaling for cancer therapy. *J. Natl Cancer. Inst.*, **94**, 1031–1032.
6. Bamford,S., Dawson,E., Forbes,S., Clements,J., Pettett,R., Dogan,A., Flanagan,A., Teague,J., Futreal,P.A., Stratton,M.R. *et al.* (2004) The COSMIC (Catalogue of Somatic Mutations in Cancer) database and website. *Br. J. Cancer*, **91**, 355–358.
7. Cogoi,S., Codognotto,A., Rapozzi,V., Meeuwenoord,N., van der Marel,G. and Xodo,L.E. (2005) Transcription inhibition of oncogenic *KRAS* by a mutation-selective peptide nucleic acid conjugated to the PKKKRKV nuclear localization signal peptide. *Biochemistry*, **44**, 10510–10519.
8. Andreyev,H.J.N., Ross,P.J., Cunningham,D. and Clarke,P.A. (2001) Antisense treatment directed against mutated Ki-ras in human colorectal adenocarcinoma. *Gut*, **48**, 230–237.
9. Kita,K., Saito,S., Morioka,C.Y. and Watanabe,A. (1999) Growth inhibition of human pancreatic cancer cell lines by anti-sense oligonucleotides specific to mutated K-ras genes. *Int. J. Cancer*, **80**, 553–558.
10. Giannini,C.D., Roth,W.K., Piiper,A. and Zeuzem,S. (1999) Enzymatic and antisense effects of a specific anti-Ki-ras ribozyme in vitro and in cell culture. *Nucleic Acids Res.*, **27**, 2737–2744.
11. Cogoi,S., Ballico,M., Bonora,G.M. and Xodo,L. (2004) Antiproliferative activity of a triplex-forming oligonucleotide recognizing a Ki-ras polypurine/polypyrimidine motif correlates with protein binding. *Cancer Gene Ther.*, **11**, 465–476.
12. Reiss,Y., Goldstein,J.L., Seabra,M.C., Casey,P.J. and Brown,M.S. (1990) Inhibition of purified p21ras farnesyl:protein transferase by Cys-AAX tetrapeptides. *Cell*, **62**, 81–88.
13. Appels,N.M., Beijnen,J.H. and Schellens,J.H. (2005) Development of farnesyl transferase inhibitors: a review. *Oncologist*, **10**, 565–578.
14. Monia,B.P., Sasmor,H., Johnston,J.F., Freier,S.M., Lesnik,E.A., Muller,M., Geiger,T., Altmann,K.H., Moser,H. and Fabbro,D. (1996) Sequence-specific antitumor activity of a phosphorothioate oligodeoxyribonucleotide targeted to human C-raf kinase supports an antisense mechanism of action in vivo. *Proc. Natl Acad. Sci. USA*, **93**, 15481–15484.
15. Sebolt-Leopold,J.S., Dudley,D.T., Herrera,R., Van Becelaere,K., Wiland,A., Gowan,R.C., Tecle,H., Barrett,S.D., Bridges,A., Przybranowski,S. *et al.* (1999) Blockade of the MAP kinase pathway suppresses growth of colon tumors in vivo. *Nat. Med.*, **5**, 810–816.
16. Yamamoto,F. and Perucho,M. (1988) Characterization of the human c-K-ras gene promoter. *Oncogene Res.*, **3**, 125–130.
17. Jordano,J. and Perucho,M. (1986) Chromatin structure of the promoter region of the human c-K-ras gene. *Nucleic Acids Res.*, **14**, 7361–7378.
18. Jordano,J. and Perucho,M. (1988) Initial characterization of a potential transcriptional enhancer for the human c-K-ras gene. *Oncogene*, **2**, 359–366.
19. Gross,D.S. and Garrard,W.T. (1988) Nuclease hypersensitive sites in chromatin. *Annu. Rev. Biochem.*, **57**, 159–197.
20. Cooney,M., Czernuszewicz,G., Postel,E.H., Flint,S.J. and Hogan,M.E. (1988) Site-specific oligonucleotide binding represses transcription of the human c-CMYC gene in vitro. *Science*, **241**, 456–459.
21. Siddiqui-Jain,A., Grand,C.L., Bearss,D.J. and Hurley,L.H. (2002) Direct evidence for a G-quadruplex in a promoter region and its targeting with a small molecule to repress c-CMYC transcription. *Proc. Natl Acad. Sci. USA*, **99**, 11593–11598.
22. Simonsson,T., Pecinka,P. and Kubista,M. (1998) DNA tetraplex formation in the control region of c-CMYC. *Nucleic Acids Res.*, **26**, 1167–1172.
23. Cogoi,S. and Xodo,L.E. (2006) G-quadruplex formation within the promoter of the KRAS proto-oncogene and its effect on transcription. *Nucleic Acids Res.*, **34**, 2536–2549.
24. Dexheimer,T.S., Sun,D. and Hurley,L.H. (2006) Deconvoluting the structural and drug-recognition complexity of the G-quadruplex-forming region upstream of the bcl-2 P1 promoter. *J. Am. Chem. Soc.*, **128**, 5404–5415.
25. De Armond,R., Wood,S., Sun,D., Hurley,L.H. and Ebbinghaus,S.W. (2005) Evidence for the presence of a guanine quadruplex forming region within a polypurine tract of the hypoxia inducible factor 1alpha promoter. *Biochemistry*, **44**, 16341–16350.
26. Sun,D., Guo,K., Rusche,J.J. and Hurley,L.H. (2005) Facilitation of a structural transition in the polypurine-polypyrimidine tract within the proximal promoter region of the human VEGF gene by the presence of potassium and G-quadruplex interactive agents. *Nucleic Acids Res.*, **33**, 6070–6080.
27. Qin,Y., REzler,E.M., Gokhale,V., Sun,D. and Hurley,L.H. (2007) Characterization of the G-quadruplexes in the duplex nuclease hypersensitive element of the PDGF-A promoter and modulation of the PDGF-A promoter activity by TMPyP4. *Nucl. Acids Res.*,, **35**, 76698–76713.
28. Phan,A.T., Kuryavyi,V., Burge,S., Neidle,S. and Patel,D.J. (2007) Structure of an unprecedented G-quadruplex scaffold in the human c-kit promoter. *J. Am. Chem. Soc.*, **129**, 4386–4392.
29. Yafe,A., Etzioni,S., Weisman-Shomer,P. and Fry,M. (2005) Formation and properties of hairpin and tetraplex structures of guanine-rich regulatory sequences of muscle-specific genes. *Nucleic Acids Res.*, **33**, 2887–2900.

30. Eddy,J. and Maizels,N. (2006) Gene function correlates with potential for G4 DNA formation in the human genome. *Nucleic Acids Res.*, **34**, 3887–3896.
31. Huppert,J.L. and Balasubramanian,S. (2007) G-quadruplexes in promoters throughout the human genome. *Nucleic Acids Res.*, **35**, 406–413.
32. Fry,M. (2007) Tetraplex DNA and its interacting proteins. *Front Biosci.*, **12**, 4336–4351.
33. Abmayr,S.M. and Worman,J.L. (1993) *Current Protocols in Molecular Biology*. John Wiley and Sons, pp. 12.1.1–12.1.6.
34. Bozzo,C, Spolaore,B., Toniolo,L., Stevens,L., Bastide,B., Cieniewski-Bernard,C., Fontana,A., Mounier,Y. and Reggiani,C. (2005) Nerve influence on myosin light chain phosphorilation in slow and fast skeletal muscles. *FEBS*, **272**, 5771–5785.
35. Perkins,D.N., Pappin,D.J., Creasy,D.M. and Cottrell,J.S. (1999) Probability-based protein identification by searching sequence databases using mass spectrometry data. *Electrophoresis*, **20**, 3551–3567.
36. Yamashita,T., Uno,T. and Ishikawa,Y. (2005) Stabilization of guanine quadruplex DNA by the binding of porphyrins with cationic side arms. *Bioorg. Med. Chem.*, **13**, 2423–2430.
37. Han,H., Langley,D.R., Rangan,A. and Hurley,L.H. (2001) Selective interactions of cationic porphyrins with G-quadruplex structures. *J. Am. Chem. Soc.*, **123**, 8902–8913.
38. Mergny,J.L., Li,J., Lacroix,L., Amrane,S. and Chaires,J.B. (2005) Thermal difference spectra: a specific signature for nucleic acid structures. *Nucleic Acids Res.*, **33**, e138.
39. Phan,A.T., Kuryavyi,V., Gaw,H.Y. and Patel,D.J. (2005) Small-molecule interaction with a five-guanine-tract G-quadruplex structure from the human MYC promoter. *Nat. Chem. Biol.*, **1**, 167–173.
40. Rujan,I.N., Meleney,J.C. and Bolton,P.H. (2005) Vertebrate telomere repeat DNAs favor external loop propeller quadruplex structures in the presence of high concentrations of potassium. *Nucleic Acids Res.*, **33**, 2022–2031.
41. Mergny,J.L. and Maurizot,J.C. (2001) Fluorescence resonance energy transfer as a probe for G-quartet formation by a telomeric repeat. *Chembiochem.*, **2**, 124–132.
42. Nazarenko,I., Pires,R., Lowe,B., Obaidy,M. and Rashtchian,A. (2002) Effect of primary and secondary structure of oligodeoxyribonucleotides on the fluorescent properties of conjugated dyes. *Nucleic Acids Res.*, **30**, 2089–2195.
43. Nagatoishi,S., Nojima,T., Galezowska,E., Juskowiaak,B. and Takenaka,S. (2006) G-quadruplex-based FRET probes with the thrombin-binding aptamer (TBA) sequence designed for the efficient fluorometric detection of the potassium ion. *ChemBioChem.*, **7**, 1730–1737.
44. De Cian,A., Guittat,L., Kaiser,M., Saccà,B., Amrane,S., Bourdoncle,A., Alberti,P., Teulade-Fichou,M., Lacroix,L. and Mergny,J.L. (2007) Fluorescence-based melting assays for studying quadruplex ligands. *Methods*, **42**, 183–195.
45. Rachwal,P.A. and Fox,K.R. (2007) Quadruplex melting. *Methods*, **43**, 291–301.
46. Phan,A.T., Modi,Y.S. and Patel,D.J. (2004) Propeller-type parallel-stranded G-quadruplexes in the human c-myc promoter. *J. Am. Chem. Soc.*, **126**, 8710–8716.
47. Dai,J., Dexheimer,T.S., Chen,D., Carver,M., Ambrus,A., Jones,R.A. and Yang,D. (2006) An intramolecular G-quadruplex structure with mixed parallel/antiparallel G-strands formed in the human BCL-2 promoter region in solution. *J. Am. Chem. Soc.*, **128**, 1096–1098.
48. Seenisamy,J., Bashyam,S., Gokhale,V., Vankayalapati,H., Sun,D., Siddiqui-Jain,A., Streiner,N., Shin-Ya,K., White,E., Wilson,W.D. *et al.* (2005) Design and synthesis of an expanded porphyrin that has selectivity for the c-*MYC* G-quadruplex structure. *J. Am. Chem. Soc.*, **127**, 2944–2959.
49. Seenisamy,J., Rezler,E.M., Powell,T.J., Tye,D., Gokhale,V., Joshi,C.S., Siddiqui-Jain,A. and Hurley,L.H. (2004) The dynamic character of the G-quadruplex element in the c-*MYC* promoter and modification by TMPyP4. *J. Am. Chem. Soc.*, **126**, 8702–8709.
50. Krishnan-Ghosh,Y., Liu,D. and Balasubramanian,S. (2004) Formation of an interlocked quadruplex dimer by d(GGGT). *J. Am. Chem. Soc.*, **126**, 11009–11016.
51. Oliviero,G., Amato,J., Borbone,N., Galeone,A., Varra,M., Piccialli,G. and Mayol,L. (2006) Synthesis and characterization of DNA quadruplexes containing T-tetrads formed by bunch-oligonucleotides. *Biopolymers*, **81**, 194–201.
52. Zhang,N., Gorin,A., Majumdar,A., Kettani,A., Chernichenko,N., Skripkin,E. and Patel,D.J. (2001) Dimeric DNA quadruplex containing major groove-aligned A-T-A-T and G-C-G-C tetrads stabilized by inter-subunit Watson-Crick A-T and G-C pairs. *J. Mol. Biol.*, **312**, 1073–1088.
53. Bugaut,A. and Balasubramanian,S. (2007) A sequence-independent study of the influence of short loop lengths on the stability and topology of intramolecular DNA G-quadruplexes. *Biochemistry*, **47**, 689–697.
54. Parkinson,G.N., Ghosh,R. and Neidle,S. (2007) Structural basis for binding of porhyrins to human telomeres. *Biochemistry*, **46**, 2390–2397.
55. Fukuda,H., Katahira,M., Tsuchiya,N., Enokizono,Y., Sugimura,T., Nagao,M. and Nakagama,H. (2002) Unfolding of quadruplex structure in the G-rich strand of the minisatellite repeat by the binding protein 1UP1. *Proc. Natl Acad. Sci. USA*, **99**, 12685–12690.
56. Han,H., Langley,D.R., Raangan,A. and Hurley,L.H. (2001) Selective interactions of cationic porphyrins with G-quadruplex. *J. Am. Chem. Soc.*, **123**, 8902–8913.
57. Comuzzi,C., Cogoi,S., Overhand,M., van der Marel,G.A., Overkleeft,H.S. and Xodo,L.E. (2006) Synthesis and biological evaluation of new pentaphyrin macrocycles for photodynamic therapy. *J. Med. Chem.*, **49**, 196–204.
58. Kraus,W.L. and Lis,J.T. (2003) PARP goes transcription. *Cell*, **113**, 677–683.
59. Akiyama,T., Takasawa,S., Nata,K., Kobayashi,S., Abe,M., Shervani,N.J., Ikeda,T., Nakagawa,K., Unno,M., Matsuno,S. *et al.* (2001) Activation of Reg gene, a gene for insulin-producing beta -cell regeneration: poly(ADP-ribose) polymerase binds Reg promoter and regulates the transcription by autopoly(ADP-ribosyl)ation. *Proc. Natl Acad. Sci. USA*, **98**, 48–53.
60. Potaman,V.N., Shlyakhtenko,L.S., Oussatcheva,E.A., Lyubchenko,Y.L. and Soldatenkov,V.A. (2005) Specific binding of poly(ADP-ribose) polymerase-1 to cruciform hairpins. *J. Mol. Biol.*, **348**, 609–615.
61. Chasovskikh,S., Dimtchev,A., Smulson,M. and Dritschilo,A. (2005) DNA transitions induced by binding of PARP-1 to cruciform structures in supercoiled plasmids. *Cytometry A.*, **68**, 21–27.
62. Tuteja,R. and Tuteja,N. (2000) Ku antoantigen: a multifunctional DNA-binding protein. *Crit. Rev. Biochem. Mol. Biol.*, **35**, 1–33.
63. Giffin,W., Torrance,H., Rodda,D.J., Prefontaine,G.G., Pope,L. and Hache,R.J. (1996) Sequence-specific DNA binding by Ku autoantigen and its effects on transcription. *Nature*, **380**, 265–268.
64. Falzon,M., Fewell,J.W. and Kuff,E.L. (1993) EBP-80, a transcription factor closely resembling the human autoantigen Ku, recognizes single- to double-strand transitions in DNA. *J. Biol. Chem.*, **268**, 10546–10552.
65. Uliel,L., Weisman-Shomer,P., Oren-Jazan,H., Newcomb,T., Loeb,L.A. and Fry,M. (2000) Human Ku antigen tightly binds and stabilizes a tetrahelical form of the Fragile X syndrome d(CGG)n expanded sequence. *J. Biol. Chem.*, **275**, 33134–33141.
66. Myers,J.C., Moore,S.A. and Shamoo,Y. (2003) Structure-based incorporation of 6-methyl-8-(2-deoxy-beta-ribofuranosyl) isoxanthopteridine into the human telomeric repeat DNA as a probe for UP1 binding and destabilization of G-tetrad structures. *J. Biol. Chem.*, **278**, 42300–42306.
67. Gagné,J.P., Hunter,J.M., Labrecque,B., Chabot,B. and Poirier,G.G. (2003) A proteomic approach to the identification of heterogeneous nuclear ribonucleoproteins as a new family of poly(ADP-ribose)-binding proteins. *Biochem. J.*, **371**, 331–340.

68. Michelotti,E.F., Michelotti,G.A., Aronsohn,A.I. and Levens,D. (1996) Heterogeneous nuclear ribonucleoprotein K is a tr.anscription factor. *Mol. Cell Biol.*, **16**, 2350–2360.
69. Bejugam,M., Sewitz,S., Shirude,P.S., Rodriguez,R., Shahid,R. and Balasubramanian,S. (2007) Trisubstituted isoalloxazines as a new class of G-quadruplex binding ligands: small molecule regulation of c-kit oncogene expression. *J. Am. Chem. Soc.*, **129**, 12926–12927.
70. Paramasivam,M., Cogoi,S., Filichev,V., Bomholt,N., Pederesen,E.B. and Xodo,L.E. (2007) Erik B. Design of twisted intercalating nucleic acids (TINA) forming antiparallel DNA triplexes with a regulatory element of the *KRAS* proto-oncogene: a new class of antigene molecules overcoming potassium problem in triplex formation. Submitted.